Analytical and Bioanalytical Chemistry (2018) 410:6585–6594
https://doi.org/10.1007/s00216-018-1263-8

RESEARCH PAPER

HILIC/ESI-MS determination of gangliosides and other polar lipid classes in renal cell carcinoma and surrounding normal tissues

Roman Hájek[1] · Miroslav Lísa[1] · Maria Khalikova[1] · Robert Jirásko[1] · Eva Cífková[1] · Vladimír Študent Jr[2] · David Vrána[3] · Lukáš Opálka[4] · Kateřina Vávrová[4] · Marcel Matzenauer[3] · Bohuslav Melichar[3] · Michal Holčapek[1]

Received: 16 May 2018 / Revised: 2 July 2018 / Accepted: 11 July 2018 / Published online: 28 July 2018

Abstract

Negative-ion hydrophilic liquid chromatography-electrospray ionization mass spectrometry (HILIC/ESI-MS) method has been optimized for the quantitative analysis of ganglioside (GM3) and other polar lipid classes, such as sulfohexosylceramides (SulfoHexCer), sulfodihexosylceramides (SulfoHex2Cer), phosphatidylglycerols (PG), phosphatidylinositols (PI), lysophosphatidylinositols (LPI), and phosphatidylserines (PS). The method is fully validated for the quantitation of the studied lipids in kidney normal and tumor tissues of renal cell carcinoma (RCC) patients based on the lipid class separation and the coelution of lipid class internal standard with the species from the same lipid class. The raw data are semi-automatically processed using our software LipidQuant and statistically evaluated using multivariate data analysis (MDA) methods, which allows the complete differentiation of both groups with 100% specificity and sensitivity. In total, 21 GM3, 28 SulfoHexCer, 26 SulfoHex2Cer, 10 PG, 19 PI, 4 LPI, and 7 PS are determined in the aqueous phase of lipidomic extracts from kidney tumor tissue samples and surrounding normal tissue samples of 20 RCC patients. S-plots allow the identification of most upregulated (PI 40:5, PI 40:4, GM3 34:1, and GM3 42:2) and most downregulated (PI 32:0, PI 34:0, PS 36:4, and LPI 16:0) lipids, which are primarily responsible for the differentiation of tumor and normal groups. Another confirmation of most dysregulated lipids is performed by the calculation of fold changes together with T and p values to highlight their statistical significance. The comparison of HILIC/ESI-MS data and matrix-assisted laser desorption/ionization mass spectrometric imaging (MALDI-MSI) data confirms that lipid dysregulation patterns are similar for both methods.

Keywords Lipids · Lipidomics · Gangliosides · Mass spectrometry · HILIC · Renal cell carcinoma · Tumor tissues

Introduction

The incidence of renal cell carcinoma (RCC) has been increasing in recent decades [1, 2]. RCC currently ranks among the ten most common cancers in industrialized countries, representing around 2% of all malignant neoplasms [1–3]. RCC originates from the renal epithelium and accounts for more than 90% of kidney tumors [4]. More than ten histological and molecular RCC subtypes have been described so far, of which clear cell RCC (ccRCC) represents an overwhelming majority of cases and accounts for most RCC-related deaths [4] with a prevalence of 75% of all primary kidney cancers [5]. Papillary and chromophobe RCC are two less common subtypes, with a prevalence of 15% of all RCC cases. Epidemiologic studies have reported an association of obesity, tobacco smoking, and hypertension with RCC [2]. The association between lipid metabolism and overall cancer risk has been suggested in many reports [6]. Abnormal metabolism of

Electronic supplementary material The online version of this article (https://doi.org/10.1007/s00216-018-1263-8) contains supplementary material, which is available to authorized users.

✉ Michal Holčapek
Michal.Holcapek@upce.cz

[1] Faculty of Chemical Technology, Department of Analytical Chemistry, University of Pardubice, Studentská 573, 532 10 Pardubice, Czech Republic

[2] Department of Urology, Faculty of Medicine and Dentistry, Palacký University and University Hospital, I.P. Pavlova 6, 775 20 Olomouc, Czech Republic

[3] Department of Oncology, Faculty of Medicine and Dentistry, Palacký University and University Hospital, I.P. Pavlova 6, 775 20 Olomouc, Czech Republic

[4] Faculty of Pharmacy Hradec Králové, Department of Organic and Bioorganic Chemistry, Charles University, Akademika Heyrovského 1203, 500 05 Hradec Králové, Czech Republic

cholesterol, phosphatidylcholines, and triacylglycerols has also been linked with the risk of RCC [7–10]. Surgery, i.e., partial nephrectomy or nephrectomy, remains the only curative therapy of RCC. Despite the progress of targeted therapy [8], including immunotherapy [9], most patients with inoperable tumors or distant metastases will eventually succumb to the disease. An early diagnosis of RCC represents a challenge, since the tumor may be asymptomatic, or the symptoms are non-specific. Although biomarkers represent an essential component in the strategy of management in the diagnosis as well as during the therapy and follow-up of many tumors [10], the utilization of biomarkers in RCC is still limited.

Lipids are diverse compounds, which may be divided according to the LIPID MAPS classification into eight major classes including fatty acyls, glycerolipids, glycerophospholipids, sphingolipids, sterol lipids, prenol lipids, saccharolipids, and polyketides [11]. Lipids play significant role in physiological processes, such as interactions between cells of the immune system, in the cellular signaling, regulation of cell apoptosis, differentiation, and transformation [12–15]. Lipids also serve as the source of energy and as building blocks of membranes [16]. In addition to the epidemiological associations between lipids and carcinogenesis, abnormal lipid metabolism is a common feature for most solid tumors and is already observed at early stages of the tumor development, for example, sulfatides are abundantly expressed in many types of cancers [15]. The lipid profile also correlates with the tumor histology and stage [17, 18], for example, sulfatide concentrations are significantly higher in malignant than in benign ovarian tumors [19]. The comparison of morphologically normal breast glandular tissue and breast tumor tissue demonstrated increased levels of fatty acids (FA) and phospholipids in tumor tissues [20], which was also reported for gangliosides [21]. Phosphatidylinositol (PI) 16:0/16:1 and PI 18:0/20:4 allow a differentiation between benign and malignant breast tumors [22]. PI 18:0/20:4, phosphatidylserine (PS) 18:0/18:1, phosphatidylglycerol (PG) 18:1/18:1, and PI 22:4/18:0 exhibit increased absolute intensities in tumor tissues of ccRCC patients, while FA 12:0 is downregulated [23].

One of the most challenging aspects in the lipidomic studies of biological samples is the evaluation of data sets of enormous size and complexity. Multivariate data analysis (MDA) workflow is typically applied for the visualization of large data sets [24] using the combination of unsupervised principal component analysis (PCA) and supervised orthogonal partial least square discriminant analysis (OPLS-DA). S-plot from supervised OPLS-DA method allows an identification of up- and downregulated lipids and a simple visualization of differences between normal and tumor samples [25–27].

The aim of this study is the differentiation of RCC tumor and surrounding normal tissues based on the hydrophilic liquid chromatography-electrospray ionization mass spectrometry (HILIC/ESI-MS) quantitation of ganglioside GM3 and other polar lipid classes (sulfohexosylceramides (SulfoHexCer), sulfodihexosylceramides (SulfoHex2Cer), PG, PI, lysophosphatidylinositols (LPI), and PS) followed by the statistical differentiation of tumor and normal groups. Unsupervised PCA and supervised OPLS-DA are used for the group differentiation, while S-plot and calculated fold changes visualize the most dysregulated lipids.

Experimental

Chemicals and standards

Acetonitrile, methanol (both HPLC/MS grade), chloroform (HPLC grade, stabilized by 0.5–1% ethanol), ammonium acetate, acetic acid, lactosyl sphingosine, cytidine-5′-monophospho-N-acetylneuraminic acid sodium salt, and α-2,3-sialyltransferase from *Pasteurella multocida* were purchased from Sigma-Aldrich (St. Louis, MO, USA). Deionized water was prepared with a Milli-Q Reference Water Purification System (Molsheim, France). Standards of SulfoHexCer d18:1/12:0 and PS 14:0/14:0 used as internal standards (IS) for the method validation and quantitation were purchased from Avanti Polar Lipids (Alabaster, AL, USA). Stock solutions of individual IS at the concentration of 1 mg/mL for GM3, SulfoHexCer, and PS were prepared in a methanol-water-chloroform mixture (6:3:1, *v*/*v*/*v*).

Samples of kidney tissues

Samples of kidney tumor and surrounding normal tissues from 20 RCC male patients (details in ESM Table S1) were obtained from the Department of Urology, Palacký University, Faculty of Medicine and Dentistry and University Hospital, Olomouc, Czech Republic. Samples were collected ca. 1 year before the measurement, and stored at − 80 °C, then transferred from the hospital to the analytical laboratory at − 20 °C, and then stored again at − 80 °C until the sample preparation. Analytical measurements were performed within few days after the extraction. The stability of this sample management was proven in our previous studies [25–27]. The study was approved by the hospital Ethical Committee, and patients signed informed consent. No sample was excluded from the statistical evaluation.

Synthesis of internal standard GM3 d18:1/12:0

3.4 mg of lactosyl sphingosine (5.45 μmol) was mixed with 1.2 mg of lauric acid (6 μmol) and 2.2 mg of 1-hydroxybenzotriazole hydrate (16.28 μmol). The mixture was dissolved in 2 mL of methanol and cooled to 0 °C using ice bath, and then 2.41 μL of N-(3-dimethylaminopropyl)-N′-

ethylcarbodiimide (13.63 μmol) was added. The cooling bath was removed, and the reaction mixture was stirred at ambient temperature for 2 days. The reaction mixture was dried with silica and purified by the column chromatography (Merck Kieselgel 60, 40–63 μm) using chloroform/methanol 2.5 mol/L ammonia (60:40:10, *v*/*v*/*v*) to yield 4.3 mg (98%) of LactosylCer d18:1/12:0 as a white solid. The product identity was confirmed by the presence of $[M+Na]^+$ and $[2M+Na]^+$ ions in positive-ion ESI mass spectra measured by Advantage Max ion-trap LCQ mass spectrometer (Thermo Finnigan, San Jose, CA, USA) and by the formation of a new spot with $R_f = 0.63$ in thin-layer chromatography (TLC) measurements using the mixture of chloroform/methanol/concentrated ammonia (60:40:12, *v*/*v*/*v*). TLC was performed on Merck aluminum sheets with silica gel 60 F254, and ammonium molybdate with ceric sulfate in sulfuric acid was used for the visualization.

4.3 mg of lactosyl ceramide (5.33 μmol) was mixed with 3.4 mg of cytidine-5′-monophospho-N-acetylneuraminic acid sodium salt (5.34 μmol) and dissolved in 1 mL of Tris buffer (pH 8, 100 mM). 2.8 mg of sodium taurodeoxycholate hydrate (5.36 μmol) was added into the resulting suspension, and the suspension was shortly sonicated to yield a cloudy solution. Using Tris buffer, the α-2,3-sialyltransferase enzyme from *Pasteurella multocida* (1 UN) was added into the solution, followed by the addition of 1 mg of $MgCl_2$ (10.5 μmol) and 100 μL of the alkaline phosphatase from bovine intestinal mucosa in Tris buffer (equivalent of 100 DEA units). The final volume of the reaction mixture was approximately 2 mL. The reaction mixture was stirred in the incubator at 37 °C and monitored by MS. After 3 h, the complete consumption of lactosyl ceramide was confirmed by MS, and the reaction was quenched. The solvent was carefully evaporated, and the residue was dissolved in methanol and dried with silica. The product was purified by the column chromatography using chloroform/methanol/2.5 mol/L ammonia (100:45:10, *v*/*v*/*v*) to yield 2.2 mg of the ganglioside GM3 (38%) as the white solid (weighed at calibrated analytical balances with the measurement for five decimal places). The product identity was confirmed by the presence of $[M+Na]^+$ ion in the positive-ion ESI mass spectrum, by the formation of the new spot with $R_f = 0.25$ in TLC measurements using the mixture of chloroform/methanol/acetic acid/water (66:25:6:3, *v*/*v*/*v*/*v*), and by the measurement under identical HILIC/ESI-MS conditions as described in the section "HILIC/ESI-MS conditions," where both chromatogram and negative-ion ESI mass spectrum show only one peak corresponding to $[M-H]^-$ ion *m*/*z* 1095.6408 wth mass accuracy 2.3 ppm (see Electronic Supplementary Material (ESM) Fig. S1). Other peaks were not observed above the background noise except for other molecular adducts. The coelution of IS and analytes from the same lipid class confirms that the structure is identical in the glycan part of the molecules, because the different structures in the glycan part would result in changed retention behavior in the HILIC mode.

Sample preparation

Human RCC tumor tissues and surrounding normal tissues were extracted according to Folch's procedure [28] with minor modifications [27, 29, 30] using chloroform/methanol/water mixture. Briefly, 25 mg of kidney tissue spiked with IS was homogenized in 6 mL of chloroform/methanol mixture (2:1, *v*/*v*) using an ultrasonic bath at 40 °C for 10 min. Then, 1200 μL of deionized water was added, and the mixture was centrifuged at 3000 rpm for 3 min. The upper aqueous layer containing polar compounds was collected, evaporated by gentle stream of nitrogen, redissolved in 1 mL of water, and finally purified by SPE. First, 200 mg of tC18 cartridge (Sep-Pak Vac, 37–55 μm particle size) (Waters, Milford, MA, USA) was conditioned with 3 mL of methanol followed by 3 mL of water. Then, 1 mL of sample dissolved in water was loaded on the cartridge, washed with 3 mL of water, and finally eluted by 3 mL of methanol. The eluate was collected, evaporated by the gentle stream of nitrogen, and redissolved in 500 μL of methanol/water/chloroform mixture (300:150:50; *v*/*v*/*v*) for the HILIC analysis. The method validation was carried out using the pooled sample prepared from all 40 kidney tissue samples collected in the present study.

HILIC/ESI-MS conditions

HILIC/ESI-MS experiments were performed on a liquid chromatograph Agilent 1290 Infinity series (Agilent Technologies, Waldbronn, Germany). The final method for the analysis of lipids used the following conditions: Ascentis Si column (150 × 2.1, 3 μm, Sigma-Aldrich), the flow rate 0.3 mL/min, the injection volume 0.5 μL, the column temperature 40 °C, and the mobile phase gradient: 0 min—95% A + 5% B, 10 min—78% A + 22% B, where phase A was acetonitrile with acetic acid, and phase B was 10 mM aqueous ammonium acetate with acetic acid (0.5 μL of acetic acid was added to 100 mL of both A and B phases).

The analytical experiments were performed on Xevo G2-XS QTOF mass spectrometer (Waters, Milford, MA, USA). Data were acquired in the sensitivity mode using negative-ion ESI using the typical resolving power 22,000 (full width at half-maximum). The acquisition range was *m*/*z* 50–2000. The capillary voltage was 1 kV, the source temperature 150 °C, the cone gas flow 50 L/h, the desolvation gas flow 1000 L/h, and the scan time 0.5 s. MassLynx Software was used for the data acquisition.

MALDI-MSI conditions

Each tissue slice for imaging experiments was immediately thaw-mounted onto stainless or microscopic glass plate and placed on the bottom side of sublimation chamber. 9-AA matrix deposition was performed in a modified sublimation apparatus described previously [31] (Chemglass Life Science, Vineland, NJ, USA) with a constant vacuum of 0.04 mbar. The stable vacuum was obtained by the rotary pump Edwards E2M28 (Edwards, Crawley, UK) supplemented with the solenoid valve DN15 (Vacuubrand, Wertheim, Germany) and controlled by the vacuum controller CVC 3000 (Vacuubrand). The sublimation time was 10 min, and temperature of oil bath was 190 °C, respectively. Mass spectra were measured using ultrahigh-resolution MALDI mass spectrometer LTQ Orbitrap XL (Thermo Fisher Scientific, Waltham, MA, USA) equipped with the nitrogen UV laser (337 nm, 60 Hz) with a beam diameter of about 80 μm × 100 μm. The LTQ Orbitrap instrument was operated in the negative-ion mode over the normal mass range *m/z* 400–2000. The long-term stability of 9-AA matrix allowed to measure images with the lateral resolution of 120 μm with the highest Orbitrap XL resolving power of 100,000 (at *m/z* 400). All experiments were performed with the automatic gain control turned off to achieve the identical number of laser shots for each pixel. Four microscans were summed for each mass spectrum (each pixel). Mass spectrometric images were generated using tissue imaging visualization software ImageQuest 1.0.1 (Thermo Fisher Scientific).

Method validation

The method validation was performed using the pooled sample prepared from 20 tumor tissues and 20 surrounding normal tissues spiked with IS. Validation parameters, such as selectivity, accuracy, carry-over, limit of detection (LOD), limit of quantitation (LOQ), and matrix effect, were determined in accordance with the European Medicines Agency (EMA) [32] recommendations, and the extraction recovery was calculated according to Food and Drug Administration (FDA) recommendations [33]. Parameters were determined for IS SulfoHexCer d18:1/12:0, PS 14:0/14:0, and GM3 d18:1/12:0 spiked into the pooled sample matrix. The selectivity was determined using six extracts of randomly selected kidney tumor tissues and surrounding normal tissues spiked before the extraction with the IS at the middle concentration level (GM3 1.2 μg/mL, SulfoHexCer 4.0×10^{-2} μg/mL, and PS 4.0 μg/mL) and six extracts of appropriate non-spiked kidney tissue samples. LOD and LOQ were determined based on signal-to-noise ratios 3 and 10, respectively. The set of nine calibration samples of IS with matrix were prepared by the dilution of IS mixture stock solution of SulfoHexCer:GM3:PS (0.1:3:9) with dilution factors of 48, 147, 312, 480, 675, 961, 1470, 1923, and 2500. Extracts of pooled sample spiked with IS before the extraction and extracts of pooled sample spiked with IS after the extraction were prepared for high-level (HL) and low-level (LL) concentrations and used to investigate the extraction efficiency. Dilution factors of IS mixture were 147 for HL (final concentrations: GM3 1.5 μg/mL, SulfoHexCer 5.2×10^{-2} μg/mL, and PS 5.2 μg/mL) and 961 for LL (GM3 0.2 μg/mL, SulfoHexCer 8.0×10^{-3} μg/mL, and PS 0.8 μg/mL), respectively. The carry-over was evaluated for each IS by the injection of blank sample with pure solvent after the injection of calibration sample at HL. The accuracy was determined for the pooled kidney sample spiked after the extraction at LL and HL concentrations. The system suitability test was evaluated as the repeatability of six injections at LL and HL concentrations, and results were calculated as the relative standard deviation (RSD, %). The matrix effect was evaluated by the comparison of the IS spiked to matrix (pooled kidney) and the pure IS.

Data analysis

Acquired data were processed using MarkerLynx XS software, i.e., individual ESI full-scans corresponding to the lipid class peak were combined together with the peak separation 50 mDa and markers extracted with the intensity threshold 3000. Then, the data in *m/z* vs. intensity format were transferred into the LipidQuant software, where concentrations of individual lipid species in nanomoles per gram are calculated using the intensity of corresponding ions in lipid class mass spectra after the isotopic correction and related to the intensity of lipid class IS. The statistical evaluation was performed by MDA methods, such as PCA and OPLS-DA in the SIMCA software (version 13.0, Umetrics, Umeå, Sweden). Data were preprocessed before the statistical analysis using the UV scaling and logarithmic transformation. Statistically significant differences were calculated using the *T* test. Fold change values were calculated from average concentrations. Box plots were plotted by Microsoft Excel 2010, and the distribution of results described values of median, minimum, maximum, and the variability of data sets using the first and the third quartiles.

Results and discussion

Synthesis of internal standard GM3 d18:1/12:0

Non-endogenous standards of GM3 are not commercially available; therefore, we have synthesized GM3 IS suitable for MS-based quantitation according to the synthesis scheme of GM3 d18:1/12:0 from lactosyl sphingosine (Fig. 1). The synthesis of GM3 started from commercially available lactosyl sphingosine. The first attempt in the synthesis was an enzymatic addition of the last sugar unit (N-

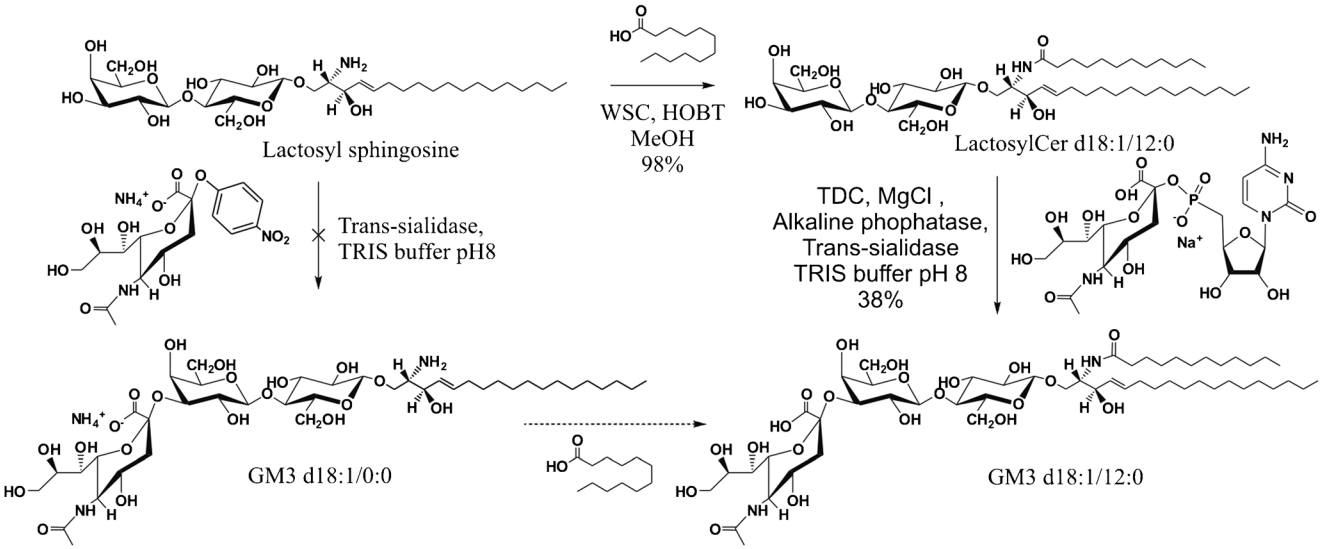

Fig. 1 Scheme of the synthesis of ganglioside GM3 d18:1/12:0 (internal standard) from lactosyl sphingosine

acetylneuraminic acid) to lactosyl sphingosine using α-2,3-sialyltransferase (trans-sialidase). N-Acetylneuraminic acid for this reaction was activated with a p-nitrophenyl group. Unfortunately, the reaction did not proceed, probably because lactosyl sphingosine with its free amino group was not a good substrate for sialyltransferase, and p-nitrophenyl was not an optimal activating group in this reaction [34].

In the second attempt, lauric acid was first linked to the free amino group of lactosyl sphingosine using water-soluble carbodiimide (WSC) and 1-hydroxybenzotriazole. This reaction proceeded almost quantitatively and provided lactosyl ceramide in a good purity. Next, N-acetylneuraminic acid was enzymatically added to lactosyl ceramide. This time, N-acetylneuraminic acid was activated using cytidine monophosphate, which was apparently better substrate for sialyltransferase, but it requires an additional enzyme (alkaline phosphatase) to cleave the phosphate bond, and magnesium cations to activate the phosphatase. Taurodeoxycholate was used to increase the lipid solubility in the buffer. Despite complete consumption of lactosyl ceramide within 3 h, the reaction gave the modified ganglioside GM3 in a 38% yield. Thus, the overall yield of this two-step synthesis was approximately 37%.

Optimization and validation

Ascentis Si column was selected for the determination of gangliosides due to the best chromatographic performance in a previous study on the characterization of gangliosides in brain tissues and other biological samples using HILIC/ESI-MS [30]. The previously used gradient conditions were optimized here to achieve the best resolution in short time for GM3 and other studied polar lipid classes, but not for other ganglioside classes [30], which were not detected in kidney tissues. The final method was validated for the quantitative analysis of GM3, SulfoHexCer, and PS in kidney tumor and surrounding normal tissues. IS were selected after the nontargeted characterization of pooled samples, because it must be absent in real biological samples. In this work, we used IS with shorter fatty acyls, such as 14:0/14:0 in case of PS and the combination of 18:1/12:0 in case of SulfoHexCer and GM3, because these combinations were not detected in the pooled sample of kidney tissues.

These IS were used for the method validation as representatives of all species within lipid classes. Pooled kidney extract spiked with the mixture of IS was used for the determination of system suitability, linearity range, calibration slope, LOD, and LOQ. The system suitability test showed acceptable

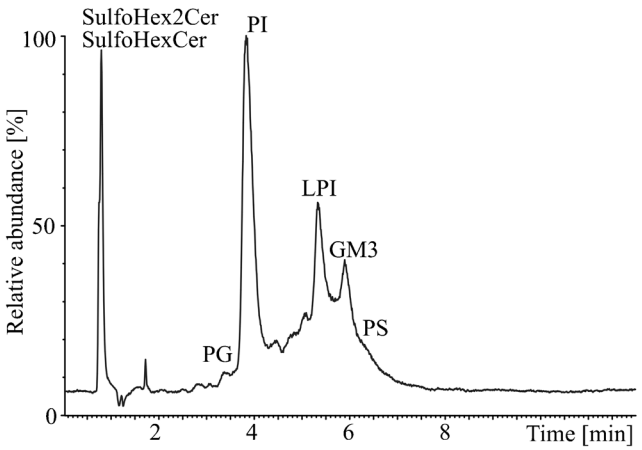

Fig. 2 Typical example of negative-ion HILIC/ESI-MS chromatogram of kidney tissue extract with the annotation of individual quantified lipid classes, including sulfohexosylceramides (SulfoHexCer), sulfodihexosylceramides (SulfoHex2Cer), phosphatidylglycerols (PG), phosphatidylinositols (PI), lysophosphatidylinositols (LPI), ganglioside (GM3), and phosphatidylserines (PS)

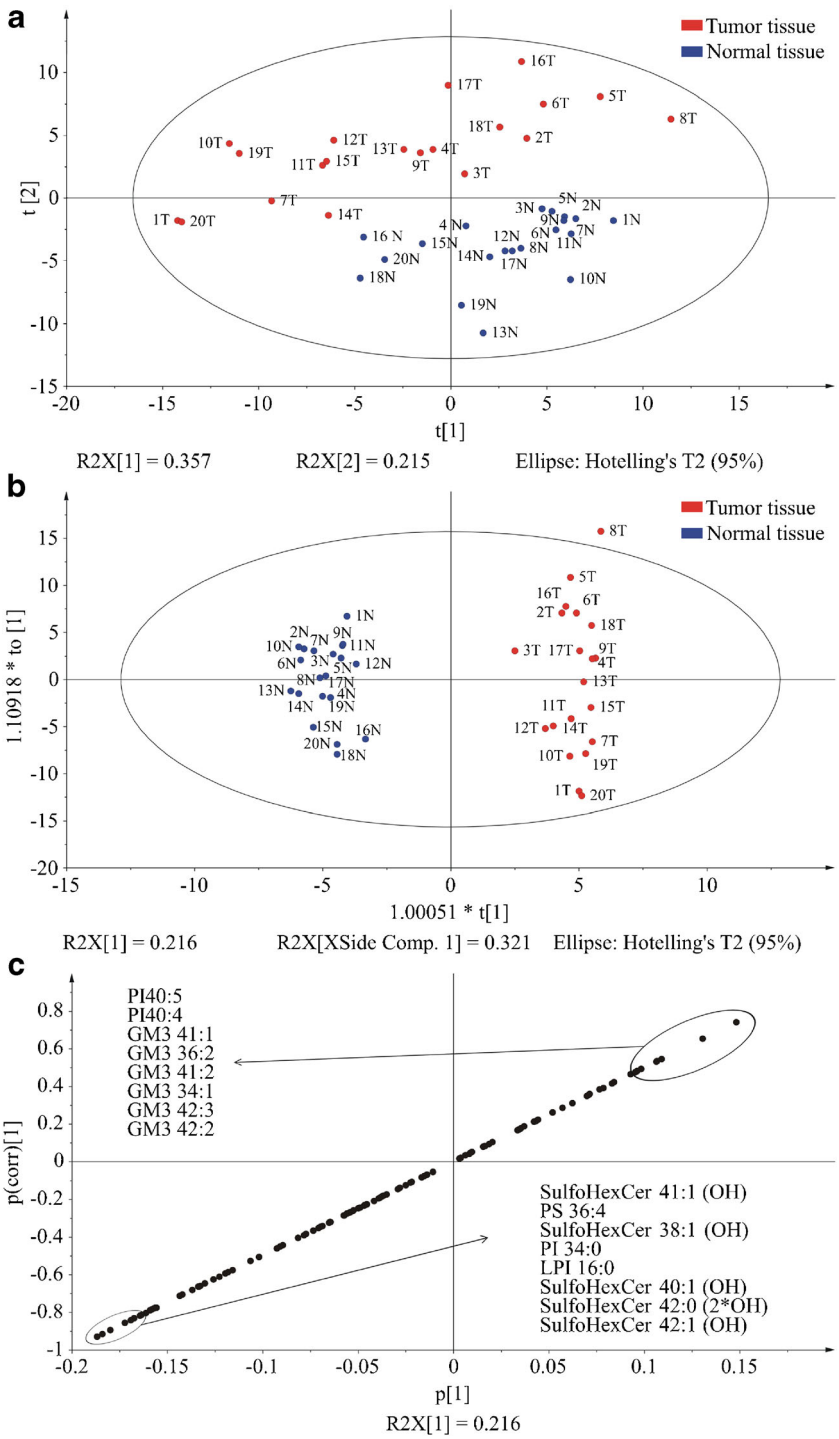

Fig. 3 Multivariate data analysis of lipidomic data for RCC tumor (red) and surrounding normal tissues (blue) measured for 20 patients. **a** Unsupervised PCA score plot. **b** Supervised OPLS score plot. **c** S-plot with the annotation of most up- and downregulated lipids

values of RSD from 2.7 to 8.1% for HL and LL (ESM Table S2). The coefficient of determination (R^2) of calibration curves was 0.9985 for SulfoHexCer, 0.9977 for GM3, and 0.9992 for PS. The matrix effect was evaluated from the analysis of pure IS and IS spiked into the pooled sample of kidney. The signal suppression was observed for SulfoHexCer (70%) and GM3 (77%). On the other hand, the ionization enhancement was observed for PS (122%). Extraction recoveries for all IS are shown in ESM Table S2 for HL and LL concentrations. PS was the most problematic class for the extraction due to its amphipathic character. The extraction recovery was around 50%, which means that 50% of PS was in the aqueous layer, and remaining 50% was in the organic layer. On the other hand, the extraction recovery of GM3 was

Table 1 Lipid species with the highest dysregulation in RCC tissues with theoretical values of their $[M-H]^-$ ions, fold changes, *T* and *p* values

	Theoretical *m/z*	Fold change	*T* value	*p* value
Upregulated lipids				
GM3 34:1	1151.7059	5.03	− 2.3	2.0E − 02
GM3 42:3	1259.7998	4.56	− 1.7	6.7E − 02
GM3 42:2	1261.8154	4.39	− 2.8	5.8E − 03
GM3 34:2	1149.6902	3.98	− 1.5	1.0E − 01
GM3 32:1	1123.6746	3.83	− 1.4	1.3E − 01
SulfoHexCer 42:3	886.6084	3.80	− 2.3	1.9E − 02
GM3 40:1	1235.7998	3.64	− 3.3	1.6E − 03
GM3 42:1	1263.8311	3.44	− 2.9	3.9E − 03
GM3 40:2	1233.7841	3.37	− 2.3	1.7E − 02
GM3 41:1	1249.8154	3.18	− 3.2	2.0E − 03
GM3 41:2	1247.7998	2.49	− 2.7	6.6E − 03
PI 40:4	913.5811	2.32	− 3.6	7.6E − 04
GM3 36:1	1179.7372	2.29	− 2.4	1.3E − 02
PI 40:5	911.5655	2.08	− 4.8	2.2E − 05
GM3 36:2	1177.7215	1.80	− 3.1	2.0E − 03
Downregulated lipids				
SulfoHexCer 42:0 (2OH)	924.6451	0.01	2.1	2.9E − 02
SulfoHexCer 41:0 (2OH)	910.6295	0.01	2.1	3.0E − 02
SulfoHexCer 40:0 (2OH)	896.6138	0.01	2.0	3.4E − 02
SulfoHexCer 41:1 (OH)	892.6189	0.01	3.4	1.3E − 03
SulfoHexCer 42:1 (2OH)	922.6295	0.03	2.1	2.8E − 02
PI 34:0	837.5498	0.03	6.6	7.0E − 07
SulfoHexCer 38:1 (OH)	850.572	0.04	4.4	1.0E − 04
SulfoHexCer 40:1 (OH)	878.6033	0.05	3.8	5.0E − 04
PS 36:4	782.4977	0.06	5.2	1.7E − 05
SulfoHexCer 42:1 (OH)	906.6346	0.07	3.6	8.3E − 04
SulfoHexCer 36:1 (OH)	822.5407	0.12	3.8	4.9E − 04
LPI 16:0	571.2889	0.18	7.3	1.0E − 07
PI 32:0	809.5185	0.19	7.2	1.1E − 08
PS 34:1	760.5134	0.20	6.9	1.6E − 07
GM3 40:1 (OH)	1251.7947	0.46	1.5	1.0E − 01

around 100%, which means that practically all GM3 were in the aqueous layer. The extraction recovery of SulfoHexCer was 70% for HL and 55% for LL. The previously developed method for brain tissues [30] was not convenient for kidney tissues, because the range of ganglioside classes was significantly lower. Therefore, the gradient conditions were optimized for this type of tissues, which also resulted in a better separation of early eluting polar lipids, such as PS, PI, LPI, and PG. Other validation parameters, such as carry-over effect, extraction recovery, selectivity, LOD, and LOQ, are summarized in ESM Table S2.

Data processing and statistical evaluation

ESM Table S1 shows the list of 20 male patients with ccRCC analyzed in the present study. RCC tumor tissue and surrounding normal tissue (classification confirmed by histology) were analyzed for each ccRCC patient. The mean (± standard deviation) age of patients was 61.7 ± 11.5 years, and the mean body mass index (BMI) was 28.9 ± 7.5 kg/m^2. ESM Table S3 lists the concentrations of 115 lipid species from seven classes determined in this study and used for further statistical evaluation with MDA methods. Individual lipids were identified based on retention times in HILIC separation (Fig. 2) and accurate *m/z* values of $[M-H]^-$ ions measured by QTOF mass analyzer with high-resolving power and high mass accuracy. The quantitative analysis of SulfoHexCer, SulfoHex$_2$Cer, GM3, and PS classes was based on the peak intensity normalized to coeluting lipid class IS. Other glycerophospholipid classes (PI, LPI, and PG) were quantified using PS 14:0/14:0 IS eluting at different retention times; therefore, the quantitative data have to be reported as

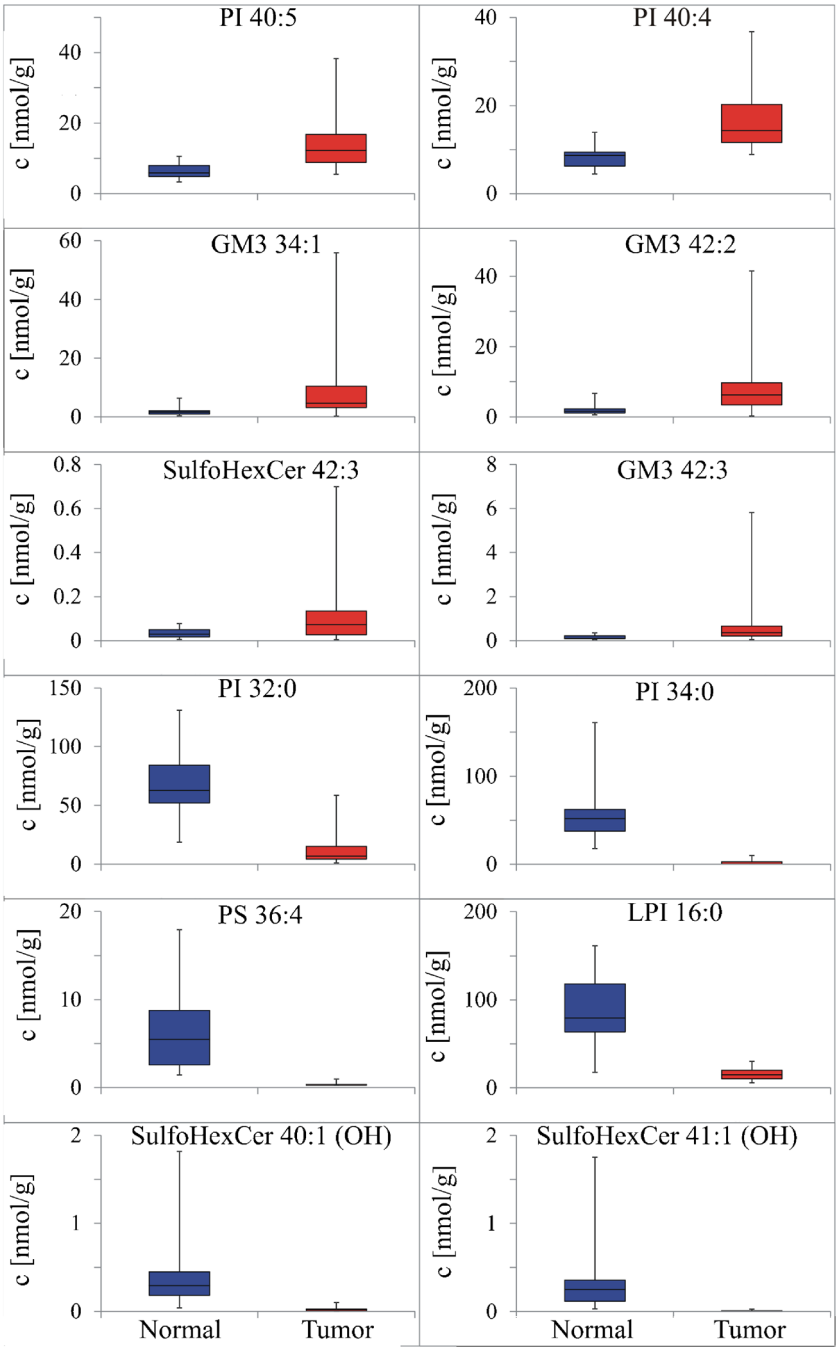

Fig. 4 Box plots of selected six upregulated (PI 40:5, PI 40:4, GM3 34:1, GM3 42:2, SulfoHexCer 42:3, and GM3 42:3) and six downregulated (PI 32:0, PI 34:0, PS 36:4, LPI 16:0, SulfoHexCer 40:1 (OH), and SulfoHexCer 41:1 (OH)) lipids in this study of 20 tumors and 20 surrounding normal tissues

semi-quantitative, although it still provides valuable information about the dysregulation of particular lipids.

MDA methods allowed the differentiation of groups of tumor and surrounding normal tissues and also the identification of the most dysregulated lipids [35]. First, the data were processed by unsupervised PCA method (Fig. 3a), which confirms the normal distribution of data set and indicates relatively good clustering of tumor samples (red points) and surrounding normal tissue samples (blue points). PCA method had six components, and the predictive ability Q2 was 0.658, where Q2 was the percent of variation of the training set—X with PCA—predicted by the model according to the cross validation. Further processing by supervised OPLS-DA (Fig. 3b) showed an excellent separation of both groups. The OPLS-DA method had 1 + 3 + 0 components, and Q2 was 0.938, where Q2 was the percent of variation of the training set—Y with OPLS—predicted by the model according to the cross validation. Q2 values larger than 0.5 indicated a high reliability of the prediction.

S-plot (Fig. 3c) created from supervised OPLS-DA method provides the information on the most upregulated (upper right part) and downregulated (bottom left part) lipids in the tumor

samples. The central part of S-plot showed lipids with a low statistical significance; therefore, they were not annotated. The most upregulated lipids in the tumor were PI 40:5, PI 40:4, GM3 41:1, GM3 36:2, GM3 41:2, GM3 42:3, GM3 34:1, and GM3 42:2, while the most downregulated ones were SulfoHexCer 41:1 (OH), PS 36:4, SulfoHexCer 38:1 (OH), PI 34:0, LPI 16:0, SulfoHexCer 40:1, SulfoHexCer 42:0 (2*OH), and SulfoHexCer 42:1 (OH). Table 1 lists 15 most up- and 15 most downregulated lipids together with their theoretical *m/z*, fold changes, *T* values, and *p* values, which specified the importance of lipids for the group clustering. The fold change was calculated from averaged concentrations in tumor and surrounding normal tissues. *p* value was calculated using *T* test and characterizes the significance level. Box plots of eight most dysregulated lipids are shown in Fig. 4 for HILIC/ESI-MS measurements, and their MS images measured by MALDI-MSI were presented in Fig. S2 (see ESM). Box plots of SulfoHexCer have been shown in our previous work measured with MALDI [35], and they are in agreement with trends reported here for HILIC/ESI-MS data (Table 1, Fig. 3c).

MALDI-MSI experiments

Similar results on dysregulated lipids were obtained by MSI of randomly selected patient, where two separated parts of tumor and surrounding normal tissues after the surgery were compared (ESM Fig. S2). All MS images representing extracted ion currents (EIC) of *m/z* values of studied lipids were reconstructed with the mass tolerance of $\Delta m/z$ 0.005. Blue to red color visualization style of changes in the lipid distribution was applied here, where the blue color represented the lowest abundance, while the red one was the highest abundance of particular EIC of deprotonated molecules of selected GM3, PI, or PS. ESM Fig. S2 shows MS images for the most dysregulated lipids identified by HILIC/ESI-MS (see box plots in Fig. 4), so the direct comparison confirms that MSI and HILIC/ESI-MS data are well correlated. Similar correlations between MALDI-MSI and HILIC/ESI-MS are obtained for other dysregulated lipids from Table 1 (not shown).

Present data indicate a potential of lipidomic studies to differentiate between RCC and normal kidney tissue. Obviously, lipidomic analysis will never be a substitute for histological diagnosis. On the other hand, lipidomic changes in the tumor could represent prognostic biomarkers as well as predictive biomarkers of response to targeted therapy, including immunotherapy. It remains to be determined how the changes in the lipidomic profile of the tumor tissue will be reflected in the concentrations of circulating lipids in body fluids. Only future prospective studies will determine whether the changes of the lipidome would be useful for early diagnosis of RCC or whether lipidomic studies will establish prognostic or predictive biomarkers in patients with early or advanced RCC.

Conclusions

Negative-ion HILIC/ESI-MS method has been optimized and fully validated in accordance with FDA and EMA recommendations for the quantitation of selected gangliosides, sulfatides, and polar phospholipids in aqueous phase of kidney tissue extracts. The present approach has been applied for the determination of 115 lipid species from seven classes (GM3, SulfoHexCer, SulfoHex2Cer, PG, PI, LPI, and PS) in 40 samples of RCC tumor tissues and surrounding normal tissues of RCC patients after the surgery. Three IS standards are used for the quantitation of GM3, both sulfatide subclasses, and PS. IS for GM3 has not been commercially available; therefore, new method for its synthesis has been developed and described here. GM3 species are strongly upregulated in tumor tissues, which can be illustrated by the fact that 11 GM3 are upregulated with the fold change higher than 2 (see Table 1). On the other hand, several sulfatides (typically with 36–42 carbons, 0–1 double bonds, and 1–2 additional hydroxyl groups) are strongly downregulated with fold changes up to 0.01, but lower *p* and *T* values show a higher variability. MDA shows a clear distinction of tumor and normal tissues (Fig. 3) using supervised OPLS-DA approach; however, the full resolution can be observed already in non-supervised PCA graph, which illustrates very significant differences of both groups based on the lipidomic analysis. Phospholipid classes PI, LPI, and PG are only semi-quantified using PS 14:0/14:0 due to the lack of their class IS, but regardless this limitation, the data show the upregulation of highly unsaturated PI 40:4 and 40:5 and the downregulation of saturated PI 32:0, PI 34:0, and LPI 16:0. The future work in this direction will continue with the analysis of gangliosides in body fluids of cancer patients together with the biological interpretation of observed changes.

Acknowledgments The help of Assoc. Prof. Jozef Škarda with the histological staining is gratefully acknowledged.

Funding information The present work was supported by ERC CZ project no. LL1302 sponsored by the Ministry of Education, Youth and Sports of the Czech Republic. K.V. and L.O. thank the support of grant project no. 16-25687J sponsored by the Czech Science Foundation.

Compliance with ethical standards

The study was approved by the hospital Ethical Committee, and patients signed informed consent.

Conflict of interest The authors declare that they have no conflict of interest.

References

1. Lee JE, Spiegelman D, Hunter DJ, Albanes D, Bernstein L, Van Den Brandt PA, et al. Fat, protein, and meat consumption and renal cell cancer risk: a pooled analysis of 13 prospective studies. J Natl Cancer Inst. 2008;100(23):1695–706.
2. Li P, Znaor A, Holcatova I, Fabianova E, Mates D, Wozniak MB, et al. Regional geographic variations in kidney cancer incidence rates in European countries. Eur Urol. 2015;67(6):1134–41.
3. Bellocco R, Pasquali E, Rota M, Bagnardi V, Tramacere I, Scotti L, et al. Alcohol drinking and risk of renal cell carcinoma: results of a meta-analysis. Ann Oncol. 2012;23(9):2235–44.
4. Hsieh JJ, Purdue MP, Signoretti S, Swanton C, Albiges L, Schmidinger M, et al. Renal cell carcinoma. Nat Rev Dis Primers. 2017;3:17009.
5. Petejova N, Martinek A. Renal cell carcinoma: review of etiology, pathophysiology and risk factors. Biomed Pap. 2016;160(2):183–94.
6. Du Y, Dun Y, Qin C, Wang X, Xu T. Preoperative serum lipid profile is associated with the aggressiveness of renal cell carcinoma. Int J Clin Exp Pathol. 2016;9:9636–40.
7. Zhang C, Yu L, Xu T, Hao Y, Zhang X, Liu Z, et al. Association of dyslipidemia with renal cell carcinoma: a 1 : 2 matched case-control study. PLoS One. 2013;8(3):e59796.
8. Buchler T, Bortlicek Z, Poprach A, Pavlik T, Veskrnova V, Honzirkova M, et al. Outcomes for patients with metastatic renal cell carcinoma achieving a complete response on targeted therapy: a registry-based analysis. Eur Urol. 2016;70(3):469–75.
9. Motzer RJ, Tannir NM, McDermott DF, Arén Frontera O, Melichar B, Choueiri TK, et al. Nivolumab plus ipilimumab versus sunitinib in advanced renal-cell carcinoma. N Engl J Med. 2018;378(14):1277–90.
10. Melichar B. Laboratory medicine and medical oncology: the tale of two Cinderellas. Clin Chem Lab Med. 2013;51(1):99–112.
11. Fahy E, Subramaniam S, Brown HA, Glass CK, Merrill AH, Murphy RC, et al. A comprehensive classification system for lipids. J Lipid Res. 2005;46(5):839–62.
12. Aureli M, Mauri L, Ciampa MG, Prinetti A, Toffano G, Secchieri C, et al. GM1 ganglioside: past studies and future potential. Mol Neurobiol. 2016;53(3):1824–42.
13. Hakomori S-I. Bifunctional role of glycosphingolipids. Modulators for transmembrane signaling and mediators for cellular interactions. J Biol Chem. 1990;265(31):18713–6.
14. Sonnino S, Mauri L, Ciampa MG, Prinetti A. Gangliosides as regulators of cell signaling: ganglioside-protein interactions or ganglioside-driven membrane organization? J Neurochem. 2013;124(4):432–5.
15. Takahashi T, Suzuki T. Role of sulfatide in normal and pathological cells and tissues. J Lipid Res. 2012;53(8):1437–50.
16. Christie WW. http://lipidlibrary.aocs.org/. Accessed Jan 2018.
17. Angerer TB, Magnusson Y, Landberg G, Fletcher JS. Lipid heterogeneity resulting from fatty acid processing in the human breast cancer microenvironment identified by GCIB-ToF-SIMS imaging. Anal Chem. 2016;88(23):11946–54.
18. Beloribi-Djefaflia S, Vasseur S, Guillaumond F. Lipid metabolic reprogramming in cancer cells. Oncogene. 2016;5(1):e189.
19. Makhlouf A, Fathalla M, Zakhary M, Makarem M. Sulfatides in ovarian tumors: clinicopathological correlates. Int J Gynecol Cancer. 2004;14(1):89–93.
20. Guenther S, Muirhead LJ, Speller AV, Golf O, Strittmatter N, Ramakrishnan R, et al. Spatially resolved metabolic phenotyping of breast cancer by desorption electrospray ionization mass spectrometry. Cancer Res. 2015;75(9):1828–37.
21. Marquina G, Waki H, Fernandez LE, Kon K, Carr A, Valiente O, et al. Gangliosides expressed in human breast cancer. Cancer Res. 1996;56(22):5165–71.
22. Yang L, Cui X, Zhang N, Li M, Bai Y, Han X, et al. Comprehensive lipid profiling of plasma in patients with benign breast tumor and breast cancer reveals novel biomarkers. Anal Bioanal Chem. 2015;407(17):5065–77.
23. Dill AL, Eberlin LS, Zheng C, Costa AB, Ifa DR, Cheng L, et al. Multivariate statistical differentiation of renal cell carcinomas based on lipidomic analysis by ambient ionization imaging mass spectrometry. Anal Bioanal Chem. 2010;398(7):2969–78.
24. Kirwan GM, Johansson E, Kleemann R, Verheij ER, Wheelock ÅM, Goto S, et al. Building multivariate systems biology models. Anal Chem. 2012;84(16):7064–71.
25. Cífková E, Lísa M, Hrstka R, Vrána D, Gatěk J, Melichar B, et al. Correlation of lipidomic composition of cell lines and tissues of breast cancer patients using hydrophilic interaction liquid chromatography/electrospray ionization mass spectrometry and multivariate data analysis. Rapid Commun Mass Spectrom. 2017;31(3):253–63.
26. Cífková E, Holčapek M, Lísa M, Vrána D, Melichar B, Študent V. Lipidomic differentiation between human kidney tumors and surrounding normal tissues using HILIC-HPLC/ESI–MS and multivariate data analysis. J Chromatogr B. 2015;1000:14–21.
27. Cífková E, Holčapek M, Lísa M, Vrána D, Gatěk J, Melichar B. Determination of lipidomic differences between human breast cancer and surrounding normal tissues using HILIC-HPLC/ESI-MS and multivariate data analysis. Anal Bioanal Chem. 2015;407(3):991–1002.
28. Folch J, Lees M, Sloane-Stanley G. A simple method for the isolation and purification of total lipids from animal tissues. J Biol Chem. 1957;226(1):497–509.
29. Ovčačíková M, Lísa M, Cífková E, Holčapek M. Retention behavior of lipids in reversed-phase ultrahigh-performance liquid chromatography–electrospray ionization mass spectrometry. J Chromatogr A. 2016;1450:76–85.
30. Hájek R, Jirásko R, Lísa M, Cífková E, Holčapek M. Hydrophilic interaction liquid chromatography–mass spectrometry characterization of gangliosides in biological samples. Anal Chem. 2017;89(22):12425–32.
31. Jirásko R, Holčapek M, Kuneš M, Svatoš A. Distribution study of atorvastatin and its metabolites in rat tissues using combined information from UHPLC/MS and MALDI-Orbitrap-MS imaging. Anal Bioanal Chem. 2014;406(19):4601–10.
32. Guideline on bioanalytical method validation. Committee for Medicinal Products for Human Use (CHMP). First published August 2011, last updated June 2015. http://www.ema.europa.eu/ema/index.jsp?curl=pages/includes/document/document_detail.jsp?webContentId=WC500109686%26mid=WC0b01ac058009a3dc.
33. FDA guidance for industry: bioanalytical method validation. US Department of Health and Human Services, Food and Drug Administration, Center for Drug Evaluation and Research: Rockville, MD. 2001. https://www.fda.gov/ForIndustry/IndustryNoticesandGuidanceDocuments/default.htm.
34. Izumi M, Shen G-J, Wacowich-Sgarbi S, Nakatani T, Plettenburg O, Wong C-H. Microbial glycosyltransferases for carbohydrate synthesis: α-2, 3-sialyltransferase from Neisseria gonorrheae. J Am Chem Soc. 2001;123(44):10909–18.
35. Jirásko R, Holčapek M, Khalikova M, Vrána D, Študent V, Prouzová Z, et al. MALDI Orbitrap mass spectrometry profiling of dysregulated sulfoglycosphingolipids in renal cell carcinoma tissues. J Am Soc Mass Spectrom. 2017;28(8):1562–74.